applied sciences

MDPI

Article

A Virtual Prototype for Fast Design and Visualization of Gerotor Pumps

Juan Pareja-Corcho [1,2], Aitor Moreno [2], Bruno Simoes [2], Asier Pedrera-Busselo [3], Ekain San-Jose [3], Oscar Ruiz-Salguero [1] and Jorge Posada [2,*]

1 Laboratory of CAD CAM CAE, Universidad EAFIT, Cra 49 no 7-sur-50, 050022 Medellín, Colombia; jpareja1@eafit.edu.co (J.P.-C.); oruiz@eafit.edu.co (O.R.-S.)
2 Vicomtech Foundation, Basque Research and Technology Alliance (BRTA), Mikeletegi 57, 20009 Donostia-San Sebastian, Spain; amoreno@vicomtech.org (A.M.); bsimoes@vicomtech.org (B.S.)
3 Egile Innovative Solutions, Kurutz-Gain Polígono Industrial Pol., 12, 20850 Gipuzkoa, Spain; asier.pedrera@egile.es (A.P.-B.); ekain.sanjose@egile.es (E.S.-J.)
* Correspondence: jposada@vicomtech.org; Tel.: +34-943-309-230

Abstract: In the context of generation of lubrication flows, gear pumps are widely used, with gerotor-type pumps being specially popular, given their low cost, high compactness, and reliability. The design process of gerotor pumps requires the simulation of the fluid dynamics phenomena that characterize the fluid displacement by the pump. Designers and researchers mainly rely on these methods: (i) computational fluid dynamics (CFD) and (ii) lumped parameter models. CFD methods are accurate in predicting the behavior of the pump, at the expense of large computing resources and time. On the other hand, Lumped Parameter models are fast and they do not require CFD software, at the expense of diminished accuracy. Usually, Lumped Parameter fluid simulation is mounted on specialized black-box visual programming platforms. The resulting pressures and flow rates are then fed to the design software. In response to the current status, this manuscript reports a virtual prototype to be used in the context of a Digital Twin tool. Our approach: (1) integrates pump design, fast approximate simulation, and result visualization processes, (2) does not require an external numerical solver platforms for the approximate model, (3) allows for the fast simulation of gerotor performance using sensor data to feed the simulation model, and (4) compares simulated data vs. imported gerotor operational data. Our results show good agreement between our prediction and CFD-based simulations of the actual pump. Future work is required in predicting rotor micro-movements and cavitation effects, as well as further integration of the physical pump with the software tool.

Keywords: digital-twin; gerotor pump; hydraulic-systems; simulation; computer-aided design

Citation: Pareja-Corcho, J.; Moreno, A.; Simoes, B.; Pedrera-Busselo, A.; San-Jose, E.; Ruiz-Salguero, O.; Posada, J. A Virtual Prototype for Fast Design and Visualization of Gerotor Pumps. *Appl. Sci.* **2021**, *11*, 1190. http://doi.org/10.3390/app11031190

Academic Editor: Andrew Y. C. Nee
Received: 16 December 2020
Accepted: 25 January 2021
Published: 28 January 2021

1. Introduction

Gerotor pumps play an important role in the aerospace industry, particularly in the processes of cooling, lubrication, and fuel boost and transfer. In other sectors, the gerotor pumps are operated in a wide range of applications, such as dosing and filling technologies in pharmacy and medicine, dispensing technologies and coating applications in manufacturing, among others. The popularity of such pumps in industrial applications arises from the fact that gerotor pumps represent a reasonable compromise in terms of compactness, reliability, cost, and versatility [1]. The working principle of a gerotor pump is based on the interaction between a pair of toothed gears with trochoidal envelope profiles. The relative movement between the profiles generates a series of chambers with varying volume that perform a cycle of suction and delivery actions (in interaction with input and output ports), thus effectively producing a volumetric flow (see Figure 1).

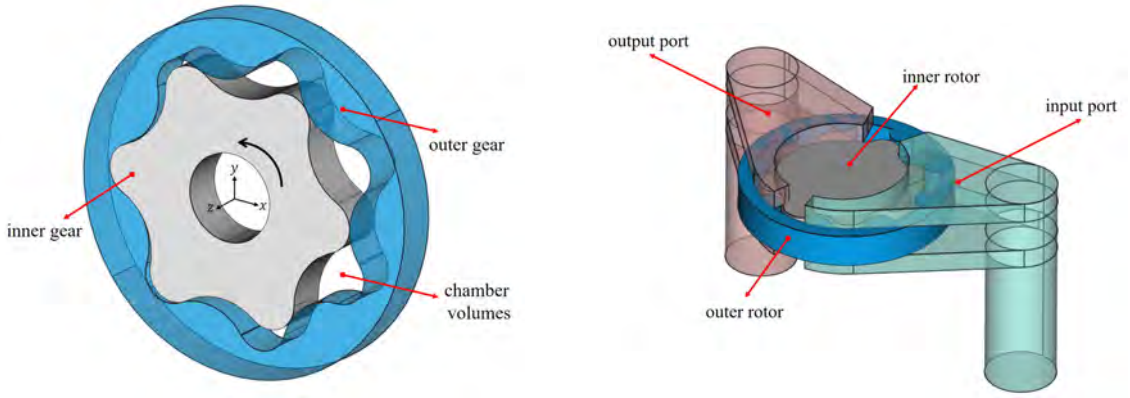

(**a**) (**b**)

Figure 1. Gerotor pump general architecture: (**a**) inner and outer gear, (**b**) inlet/outlet disposition in pump.

The current design process for gerotor pumps commonly involves: (i) a *geometric modeling* step in a CAD environment, (ii) a *design verification* phase using fluid mechanics simulations to validate the efficiency and other desired characteristics of the pump, and (iii) a *physical testing* phase to verify the predicted characteristics of the pump in a real test bench once the design has been validated through a simulation tool. This process can be considerably time-consuming, due to the large amount of time that is required in the design verification stage. The design engineer must mesh the complex geometry of the volume chambers each time that the design is changed and perform a time-consuming simulation. In most design cases, the simulation of a geometric configuration takes up to a day to generate results. The described workflow hinders the effectiveness of rapid design methodologies or the easy testing of a large number of geometric configurations of the pump in a reasonable time.

Implementation. In this manuscript, we present the implementation of a virtual prototype of a Gerotor pump designed to be integrated with data measured in an experimental setup in order to improve the established design process. Our implementation does not constitute a full Digital Twin, but rather will be a step towards a fully functional Digital Twin tool that reproduces the behavior of the real pump. This virtual prototype allows for a rough design condition vs. performance appraisal, thus enabling the design and testing scenarios. Once the designer is satisfied with this approximated design vs. performance ratio, a more precise CFD simulation process would take place. An important current feature of the virtual prototype tool presented is the import and display of the sub-sequent CFD simulation results and experimental data measured in a real pump, for the benefit of the designer manufacturer and client. This feedback of the CFD simulation results might be included in a numerically oriented closed loop at the design stage. At the present time, we only report visual CFD data feedback. The implemented tool is able to use data that were measured in the experimental setup to feed the fast virtual prototype. Differences between the virtual prototype state variables and measured state variables allow for several activities: (a) to modify the pump design, (b) to control the actual pump, and (c) to feed satisfactory virtual prototype parameters into parametric or constraint-driven CAD models to obtain a full Boundary Representation of the Gerotor pump. Notice that (c) streamlines the design-for-gerotor process and avoids the need for a external CAD application.

The manuscript is divided, as follows: the Section 2 reviews the available literature in the context of physical simulation of gerotor pumps and Digital Twin implementations. Section 3 introduces the experimental setup of the pump, the lumped parameter model, and the virtual prototype tool. Section 4 presents the comparison between our predictions and a Computational Fluid Dynamics simulation used as ground truth. We do not address the comparison with respect to the experimental data, because we cannot measure the comparison variable in our experimental setup. Section 5 concludes the manuscript and

discusses possible future developments in both the virtual prototype and its integration within a full Digital Twin tool.

2. Previous Works

In this section, we review the literature in two dimensions: (a) methods for fluid dynamics simulation in gerotor pumps and (b) implementations of virtual prototypes in Digital Twin oriented tools.

2.1. Fluid Mechanical Simulation

Several approaches have been proposed to simulate the performance of gerotor pumps, depending on the level of detail required. Most previous work relies on two methods for the fluid simulation: (i) lumped parameters models (LP) and (ii) computational fluid dynamics models (CFD), with each one exhibiting different performances regarding time and memory complexity.

CFD models: computational fluid dynamics models use specialized software to solve the Navier–Stokes equations in a discretized domain. CFD models can be classified in two categories: (i) two-dimensional (2D) models and (ii) three-dimensional (3D) models. Castilla et al. [2] and Houzeaux et al. [3] presented 2D CFD models for the simulation of rotary pumps that present accurate results with respect to an experimental setup. Recently, 3D simulations of the pump have been performed in order to analyze specific aspects of the pumps design, such as: (a) profile geometry optimization [4,5], (b) discharge coefficient calculation [6], and (c) fluid leakage due to clearances [7]. The main advantages of CFD based methods are: (i) detailed description of the fluid's behavior inside the cavity of the pump and (ii) very accurate prediction of the effect of cavitation and fluid–body interaction on performance. The main disadvantages of CFD methods are: (i) large simulation time and memory requirements, (ii) the requirement to remesh the entire domain in each step of the solution, and (iii) the difficulty to mesh appropriately the inter-teeth clearance domain [2].

LP models: lumped parameter models discretize the pump in a number of control volumes, where each CV (control volume) corresponds to a cavity of the pump. The mass and energy conservation equations are used to integrate the pressure in each control volume. The pressure inside each control volume will depend on the instantaneous volume of the chamber and net flowrate of fluid through its surface. Pellegri et al. [8,9] presented a simple lumped parameter model that was mounted on AMESIM software, coupled with a geometric module that calculates the instantaneous areas and volumes of the chambers. The results show good agreement between predicted and measured data. Shah et al. [10] presented a lumped parameter model in AMESIM software for the prediction of cavitation effects on the pump simulation; the results show that the model is accurate in predicting the effect of cavitation phenomena on the overall performance of the system. The main advantages of the lumped parameter approach are: (i) the low time and memory complexity and (ii) the flexibility to integrate with larger hydraulic circuits [1,8,9]. The main disadvantages of the lumped parameter approaches are: (i) the results are coarse with respect to CFD methods and (ii) calibration of the model vs. experimental data is needed, which makes this approach unsuitable for detailed analysis of local behavior of fluid [11].

2.2. Digital Twins and Virtual Prototypes in Gerotor Applications

Digital Twins are virtual abstractions of physical products, processes, or phenomena very commonly used in the context of Industry 4.0 [12]. Digital Twins are a valuable tool in digital design and manufacturing, as they allow for prediction of system performance and simulation/optimization. Relatively few applications of Digital Twin methodology are found in industrial contexts [13], opening opportunities for wider adoption of Digital Twins in industries, such as fluid power systems. The use of accelerated coarse simulations for fast decision making, although not being entirely similar to the concept of Digital Twin, is being explored in other industrial contexts, such as quality control in manufacturing [14,15].

The lumped-parameter models that have been cited in the previous sections are usually implemented in specialized commercial software. This restriction limitates their feasibility towards a fully functional Digital Twin tool that integrates data from an experimental test bench. In the case of lumped parameter models, the design engineer must express the pump in a CAD environment and then import the geometric data into a differential equation solver (e.g., AMESIM [9]). In the case of CFD models, several commercial codes are used in the solution of the Navier–Stokes equations, including PumpLinux, ANSYS Fluent, and CFX (all appearing in Ref. [11]). So far, we have found no standalone fully-integrated implementations of gerotor pump simulation environments that suits our design needs.

2.3. Conclusions of Literature Review

Two approaches are commonly used in the context of gerotor pump simulation: (i) Lumped Parameter (LP) models and (ii) Computational Fluid Dynamics (CFD) models. The lumped parameter models allow for the fast simulation of pump performance at the price of loss of accuracy and detail. CFD models allow for very accurate simulation of pump performance with detailed information regarding in-chamber heterogeneity, at the expense of large simulation time and complexity. Because of its accuracy, it is common to use CFD as a ground truth value for pump experiments when no experimentally obtained comparison data are available. We use CFD as our point of comparison for the reasons expressed above and the availability of CFD software simulation. Furthermore, we found that implementations of both approaches are: (i) dependant on proprietary commercial software and (ii) not easily integrated with other standalone non-commercial design and optimization tools in the context of Digital Twins tools.

As a response to such shortcomings, we present the implementation of a virtual prototype for a gerotor pump, which also allows for the integration of measured data, thus enabling the functioning of a Digital Twin. Our implementation: (1) integrates pump design, fast approximate simulation, and result visualization processes, (2) does not require an external numerical solver platforms for the approximate model (as other approaches do), (3) allows for the fast simulation of gerotor performance, and (4) feeds the simulation model with data measured in an experimental setup to improve the accuracy of the model. Several variables can be used to assess the pump behavior, including, among others, maximum pressure, torque, and power. We use the maximum pressure in the pump as our comparison variable since (1) it is a variable of interest for the pump manufacturer and the variable that our model predicts and (2) the comparison with other variables (e.g., torque) would require specialized proprietary software. This software is not available to the industry manufacturer. See Implementation in the Introduction section.

3. Methodology

For our Digital Twin (DT) implementation, we have defined a three step workflow: (i) the design engineer inputs the values for the parameterization of pump design into the Geometry Configurator, (ii) the geometric model of the pump (inner and outer gears) is generated, and (iii) the virtual prototype performs the fast simulation of the pump with the geometric data and experimental data being measured from the test bench (see Figure 2). Please see the Abbreviations section immediately before the References section to find the meaning for the symbols used.

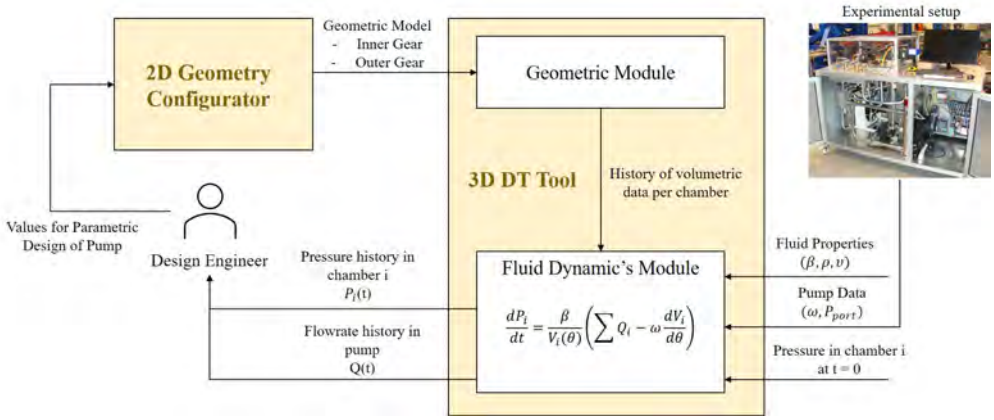

Figure 2. Implemented Tool Architecture and Workflow.

This section is divided in three parts: (1) we present the experimental setup where we show the data collection setup used to feed the virtual prototype tool, (2) we explain the geometric model, showing the generation of the gerotor geometric model and the calculation of geometric quantities such as the history of chamber volumes and areas, (3) we present the fluid dynamics module, where we lay out the foundations of the simulation model and (4) we discuss the software tool that integrates the virtual prototype model, including 3D visualization, with the data being collected from the experimental setup and external CFD simulations.

3.1. Experimental Setup

The contact point between the physical pump and the computational modeling is the testing bench. The experimental setup hosts the sensors that are used to collect performance data and feed it to the simulation model. Figure 3 presents the testing bench setup used and a manufactured pump mounted in the bench with a translucent cover.

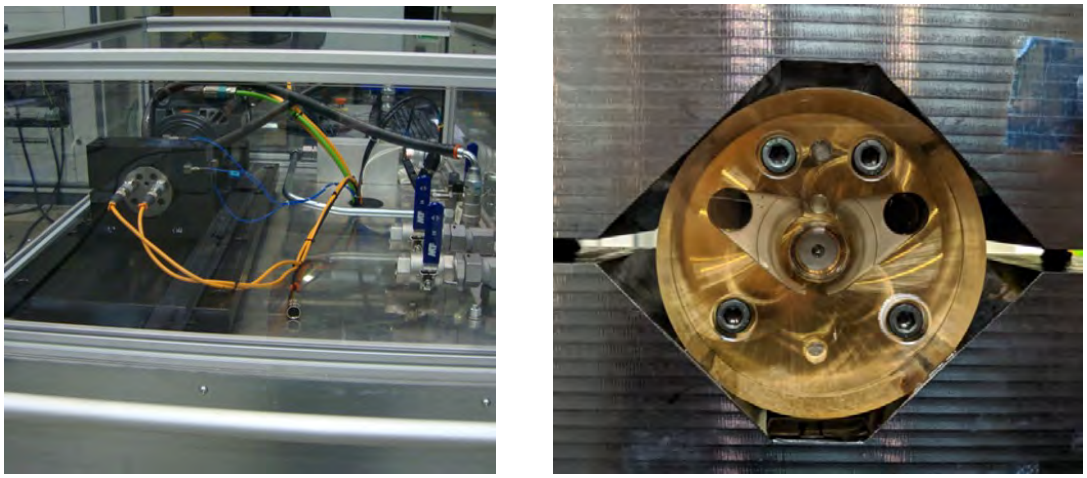

(**a**) (**b**)

Figure 3. Experimental setup: (**a**) testing bench and (**b**) physical pump mounted on the test setup (translucent cover).

Pressure sensors that are located in the input and output ports measure the pressure value to be fed to the virtual prototype (as shown in Figure 2). Further integration of the data that were collected in the testing bench for variables other than pressure with the simulation model is still to be addressed.

3.2. Geometric Model

The internal profile of the gerotor is generated according to the parameterization proposed by Ref. [16]:

$$x_i(\alpha_{pc}) = R_2 \cos\left(\frac{1}{Z-1}\alpha_{pc}\right) \pm e\cos\left(\frac{Z}{Z-1}\alpha_{pc}\right) - \frac{S}{m}\left[R_2\cos\left(\frac{1}{Z-1}\alpha_{pc}\right) \pm r_2\cos\left(\frac{Z}{Z-1}\alpha_{pc}\right)\right] \quad (1)$$

$$y_i(\alpha_{pc}) = -R_2 \sin\left(\frac{1}{Z-1}\alpha_{pc}\right) \mp e\sin\left(\frac{Z}{Z-1}\alpha_{pc}\right) + \frac{S}{m}\left[R_2\sin\left(\frac{1}{Z-1}\alpha_{pc}\right) \pm r_2\sin\left(\frac{Z}{Z-1}\alpha_{pc}\right)\right] \quad (2)$$

$$m = \sqrt{r_2^2 + R_2^2 \pm 2r_2R_2\cos\alpha_{pc}} \quad (3)$$

where the parameter $\alpha_{pc} \in [0, 2\pi]$ corresponds to the turning angle of the rotor. Figure 4 shows the resulting shape of the internal profile as the trace of contact point P', whose position is determined by the radii R_2 and r_2, the eccentricity e, and the number of chambers Z. In Figure 4, the external profile is determined by a set of outer circumferences that are truncated by a larger cutting circumference.

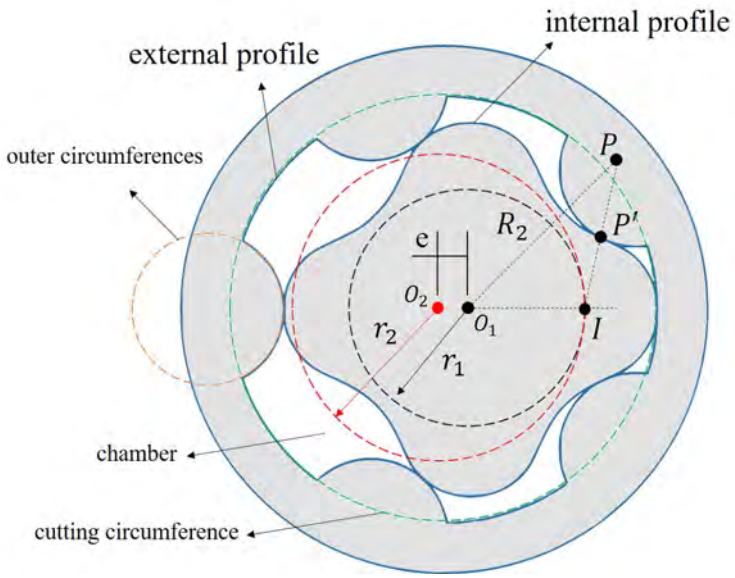

Figure 4. Parameterization of internal profile shape as in Equation (2).

This construction method of the external profile, even though simple and widely used, limits the performance of the pump, as the resulting shape does not mesh perfectly with the internal profile shape [17]. We have implemented an additional method to build the external profile as the conjugated curve of the internal shape.

Suppose the curve C that corresponds to the internal profile (Equations (1) and (2)) is put through a series of affine transformations that are defined by the rolling without slipping of the circumference defined by r_1 with respect to the circumference defined by r_2 in Figure 4. Subsequently, the external profile shape will be defined as the envelope curve of the locus of C as it moves through the rotation domain.

Figure 5 shows the locus of curve C, as generated by the movement of the circumferences. The envelope curve of the locus can be used as the external profile shape, with the advantage that by using this external shape both curves mesh perfectly, hence improving the performance by avoiding fluid recirculation. Once the inner and outer profile shapes are defined, the geometric quantities of each chamber are calculated by sampling both the internal and external curve to form a closed polygon, finding the area A_i and perimeter P_i of the polygon corresponding to chamber i.

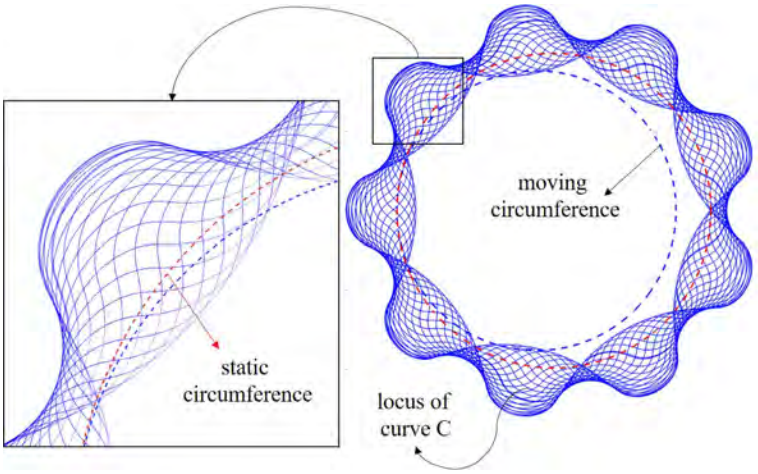

Figure 5. Locus of the internal profile curve *C*.

3.3. Fluid Dynamics Module

We discretize the flow domain in several control volumes to obtain a lumped parameter model of the pump, as shown in Figure 6. We assume the fluid properties within each control volume (CV) to be homogeneous, but not constant in time, effectively treating each control volume as the basic domain of simulation. Notice that, as the pump rotates, the geometry of the control volumes changes; therefore, the model requires a constant update of the geometric calculations for each control volume (area, perimeter) as the position of the pump changes (see Figure 2).

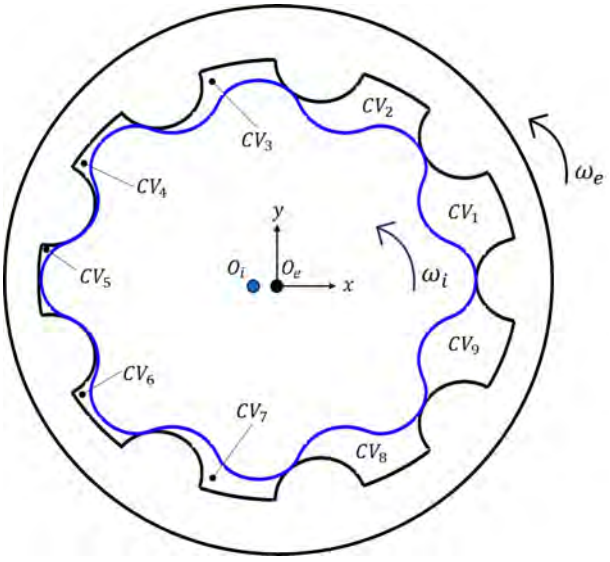

Figure 6. Control Volume discretization of the gerotor pump.

By the principle of the conservation of mass and energy, along with Reynold's transport theorem, it is possible to derive an expression for the change of pressure within a control volume:

$$\frac{dp}{dt} = \frac{\beta_{eff}(p)}{V(\theta)}\left(\sum Q_i - \omega\frac{dV}{d\theta}\right) \tag{4}$$

We omit the derivation of such an expression, since it is beyond the scope of our paper, the interested reader can find a thorough explanation in Ref. [11]. The net flowrate that flows through the boundary of a control volume needs to be calculated in order to integrate Equation (4), and since the volume and volume derivative at angle θ are provided by the

geometric module. We consider two types of flows through the boundary of a control volume (Figure 7):

1. *Input/Output flow*: fluid flowing from the input port to the inside of the pump (charge) or from the inside of the pump to the output port (discharge).
2. *Fluid leak flow*: fluid flowing from one chamber to another due to imperfect sealing that results from manufacturing defects and design constraints.

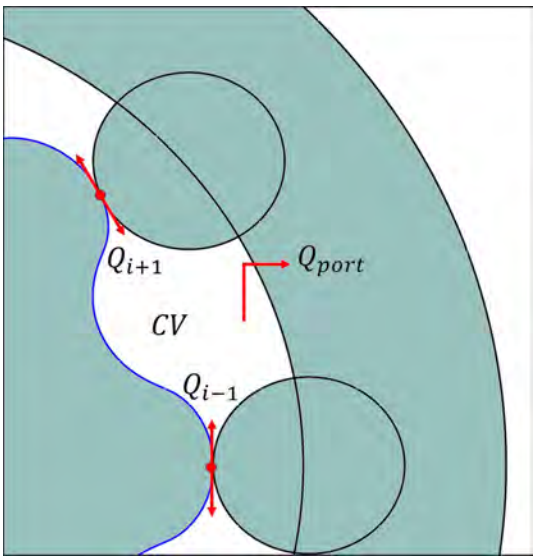

Figure 7. Types of flows through the boundary of a control volume.

The flow between the control volume and the input/output port is modeled as the flow through a variable geometry orifice subject to a difference in pressure. The pressure at the input and output ports is fed to the numerical model with data that were collected from the experimental testing bench, while the control volume pressure varies according to Equation (4). The flowrate in this situation can be obtained as:

$$Q_{in} = C_d A_{i,in} \sqrt{\frac{2(P_i - P_{in})}{\rho_{eff}}} \tag{5}$$

$$Q_{out} = C_d A_{i,out} \sqrt{\frac{2(P_i - P_{out})}{\rho_{eff}}} \tag{6}$$

Notice that, since a control volume only interacts with one of the ports at any given time, the net port flowrate Q for a control volume is equal to Q_{in} or Q_{out}, depending on the position of the control volume at the time of analysis. The calculation of the discharge coefficient C_d depends on the value of the Reynold's number Re and the hydraulic diameter D_h at such a time. The hydraulic diameter D_h and the Reynold's number Re are calculated, as follows:

$$D_h = \frac{4A_i(\theta)}{P_i(\theta)} \tag{7}$$

$$R_e = \frac{D_h}{\nu} \sqrt{\frac{2\Delta P}{\rho_{eff}}} \tag{8}$$

Finally, the discharge coefficient C_d is estimated while using an experimental expression (Ref. [11]):

$$C_d = C_{d\,\max} \tanh\left(\frac{2R_e}{R_{ecrit}}\right) \tag{9}$$

where $C_{d\,\max}$ is the maximum discharge coefficient and R_{ecrit} is the critical Reynolds number, which indicates the transition between laminar and turbulent regime. Values for constants $C_{d\,\max}$ and R_{ecrit} can be found in the literature as a function of conditions of the pump [8]. This flow between adjacent control volumes that should be nominally tight is enabled by the small gap between the rotors at their maximal approximation position. These gaps are necessary for ensuring rotation and limit friction and wear. The resulting fluid migration between adjacent chambers is caused by:

1. Difference of pressure between adjacent control volumes (Poiseuille flow).
2. Difference in angular speed between inner and outer rotor (Couette flow).

Typically, the gap between rotors at contact points is very small when compared to the overall size of the pump. The curvature radii at the throat are much larger than the throat gap. Therefore, (1) and (2), above, may be modeled by assuming that the approaching teeth form a constant clearance gap between two parallel plates (Figures 8 and 9).

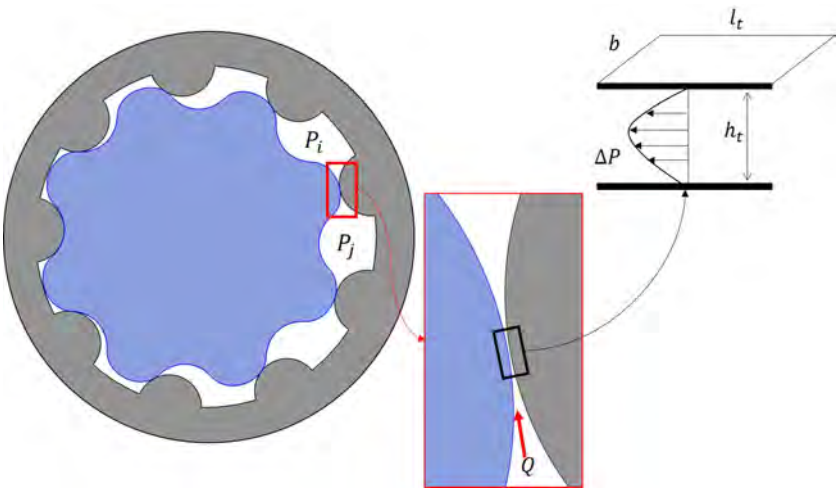

Figure 8. Pouiseuille flow between adjacent control volumes.

Figure 8 shows the working principle of the Poiseuille flow in the pump case, where two static plates of length l_t and width b are separated by a distance h_t. The difference in pressure between adjacent control volumes induces a flow Q_p that can be obtained as:

$$Q_p = b\frac{\Delta P(\frac{h_t}{2})^3}{12\mu L} \tag{10}$$

Notice that width b corresponds to the length of the pump profiles in the z direction. The distance h_t is estimated by the geometric module as it may vary for each contact point throughout the rotation of the rotors. As length l_t cannot be directly measured in the geometric model, we estimate l_t as a function of h_t. Starting from the point of minimum distance h_t, we move outwards through the profile curves to the point where the distance between rotors is $h_t* = (1+\epsilon)h_t$. Once such points are found, the length l_t is assumed to be the Euclidean distance between the points found. This approximation has shown to be effective for values of ϵ around 0.1 [8].

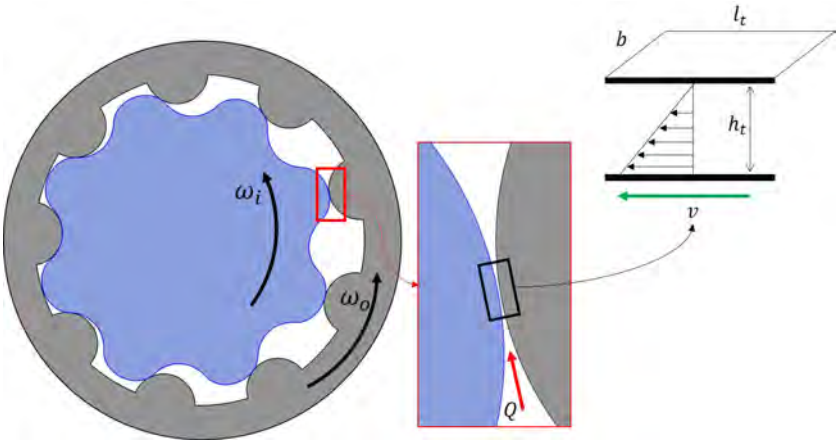

Figure 9. Couette flow between adjacent control volumes.

Figure 9 shows the working principle of the Couette flow. Two parallel plates having relative velocity with respect to each other produce a flowrate between them through the viscosity of the fluid and shear stress induced by the relative movement of the plates. The Couette and Poiseuille flows (Figures 8 and 9) both result in a fluid exchange between adjacent control volumes, therefore affecting the net flowrate through their borders and their pressures. Finally, as the pump usually operates in a low pressure range, the variance of effective fluid properties (bulk modulus, density) in hydraulic oil with respect to the instantaneous pressure [18] inside a control volume must be taken into account:

$$\beta_{\text{ef}} = \frac{\beta_{\text{oil}}}{1 + \alpha \cdot \left(\frac{p_0}{p}\right)^{\frac{1}{k}} \cdot \left(\frac{\beta_{\text{oil}}}{\kappa \cdot p} - 1\right)} \tag{11}$$

$$\rho_{\text{ef}} = \frac{\alpha \cdot \rho_{\text{air},0} + (1-\alpha) \cdot \rho_{\text{oil},0}}{\alpha \cdot \left(\frac{p_0}{p}\right)^{\frac{1}{K}} + (1-\alpha) \cdot \left(1 + \frac{m \cdot (p - p_0)}{\beta_{oil}}\right)^{-\frac{1}{m}}} \tag{12}$$

where β_{oil}, ρ_{air}, and ρ_{oil} are the properties of the oil and air at atmospheric conditions, respectively. p_0 is the atmospheric pressure, α is the void fraction, and κ is the polytropic constant of air.

3.4. Software Tool

The Digital Twin (DT) tool implements two functionalities: a *2D geometry configurator* and a *3D data tool*. The 2D geometry configurator allows for the design engineer to define a new geometry for the profiles of the inner and outer gears according to a set of parametric variables. The 3D data tool converts the model that is defined in the 2D geometry configurator to a full B-Rep model for simulation and visualization purposes of both (i) data simulated from our pre-CFD simulation model and (ii) data imported from CFD simulations or test bench.

Figure 10 shows the visualization of the parameterized pump in the interface of the 2D geometry configurator tool. The tool allows for the design engineer to input the desired set of values for the parametric variables of Equation (2). Our application automatically generates both the conjugated design (Figure 10a) and the classic design (Figure 10b). Both types of design, as well as other geometric configurations, are easily explorable in the 2D visualization canvas.

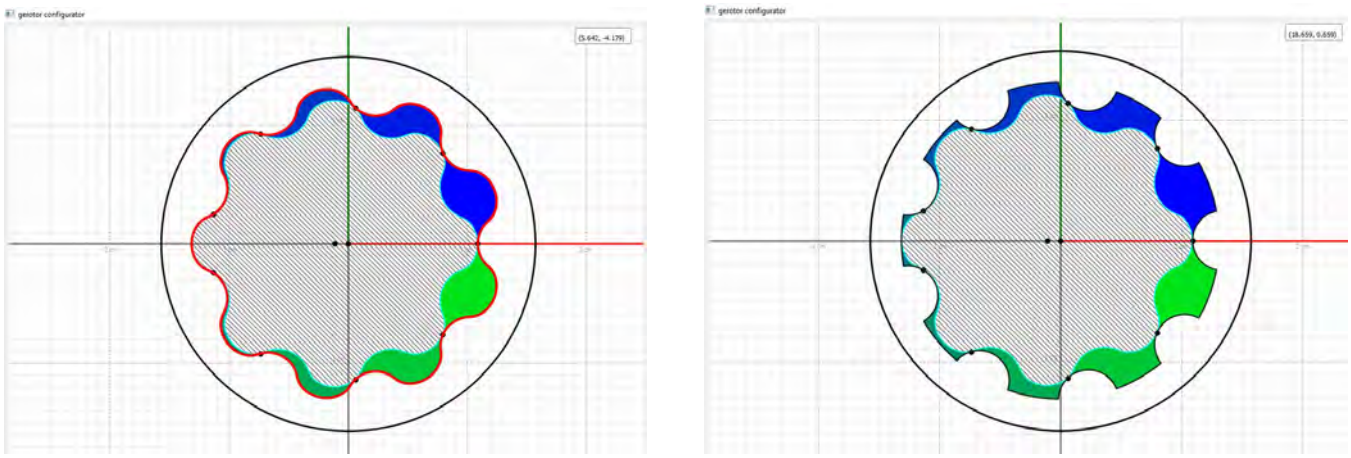

(**a**) (**b**)

Figure 10. Visualization of parameterized pump in the two-dimensional (2D) geometry configurator interface: (**a**) pump with conjugated external profile and (**b**) pump with classic external profile.

In addition to the discretized geometric model of the inner and outer gears, the geometry configurator calculates the shape of the resulting chambers for any given angle of the rotation of the pump. The configurator allows the user to interactively rotate the pump position with a slider, as well as to visualize and record the change in the area of each one of the chambers.

The ports and chambers geometries must be well-aligned for the correct calculation of the intersection area between the chambers and the ports. The geometry of the input/output ports (shown in Figure 11) of the pump is calculated from the geometry of the inner and outer gear geometries in order to ensure the alignment. The geometries calculated by this application (gear, chamber, and port geometry) are automatically imported into the 3D data tool for simulation purposes. The CAD models are also exported to external files.

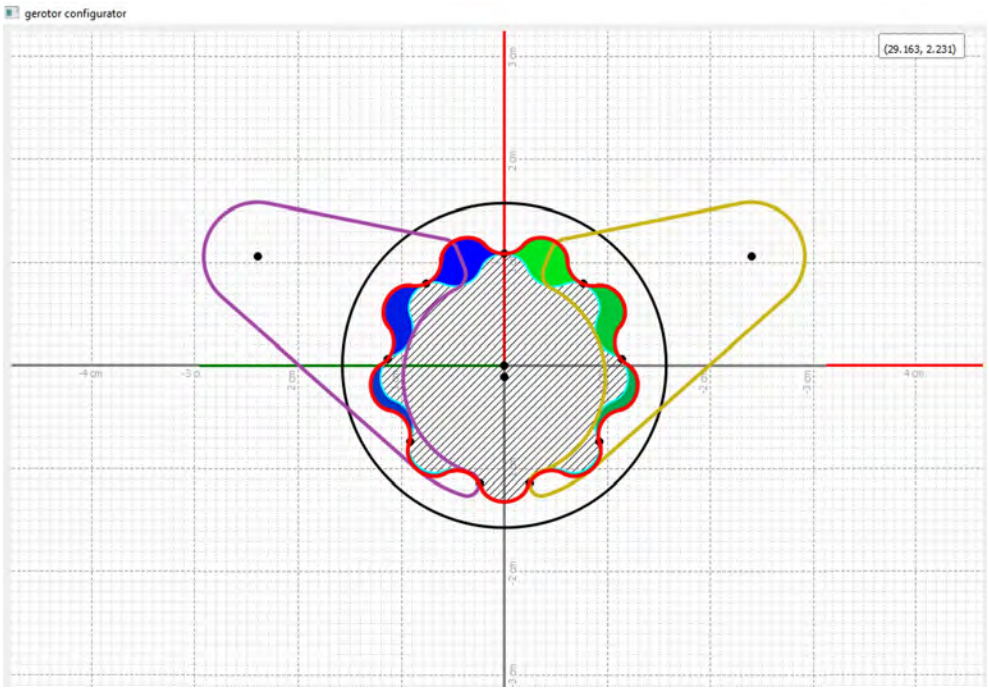

Figure 11. Gerotor design with input/output ports.

Figure 12 shows the interface that is devised for the toolkit that was introduced in [19,20] to enable the virtual prototype. The interface is built with Qt™ library and it comprises several panels: (i) the *3D visualization panel*, which allows for the visualization of the pump geometry (gears, ports, and chambers) and the animation showing the rotation of the pump through a pumping cycle, (ii) a *hierarchy panel* that shows the hierarchy tree of the geometric model and allows the user to select and highlight geometric entities, (iii) a *settings panel* in which the user inputs the fluid properties, operating conditions, and initial pressure conditions that are necessary to perform the fast pre-CFD simulation (see Figure 2), (iv) a *simulated data panel* that displays the results from the fast simulation model, and (v) a *measured data panel* that displays the results of the variables that are imported to the virtual prototype tool, whether measured in the test bench or simulated by the CFD software.

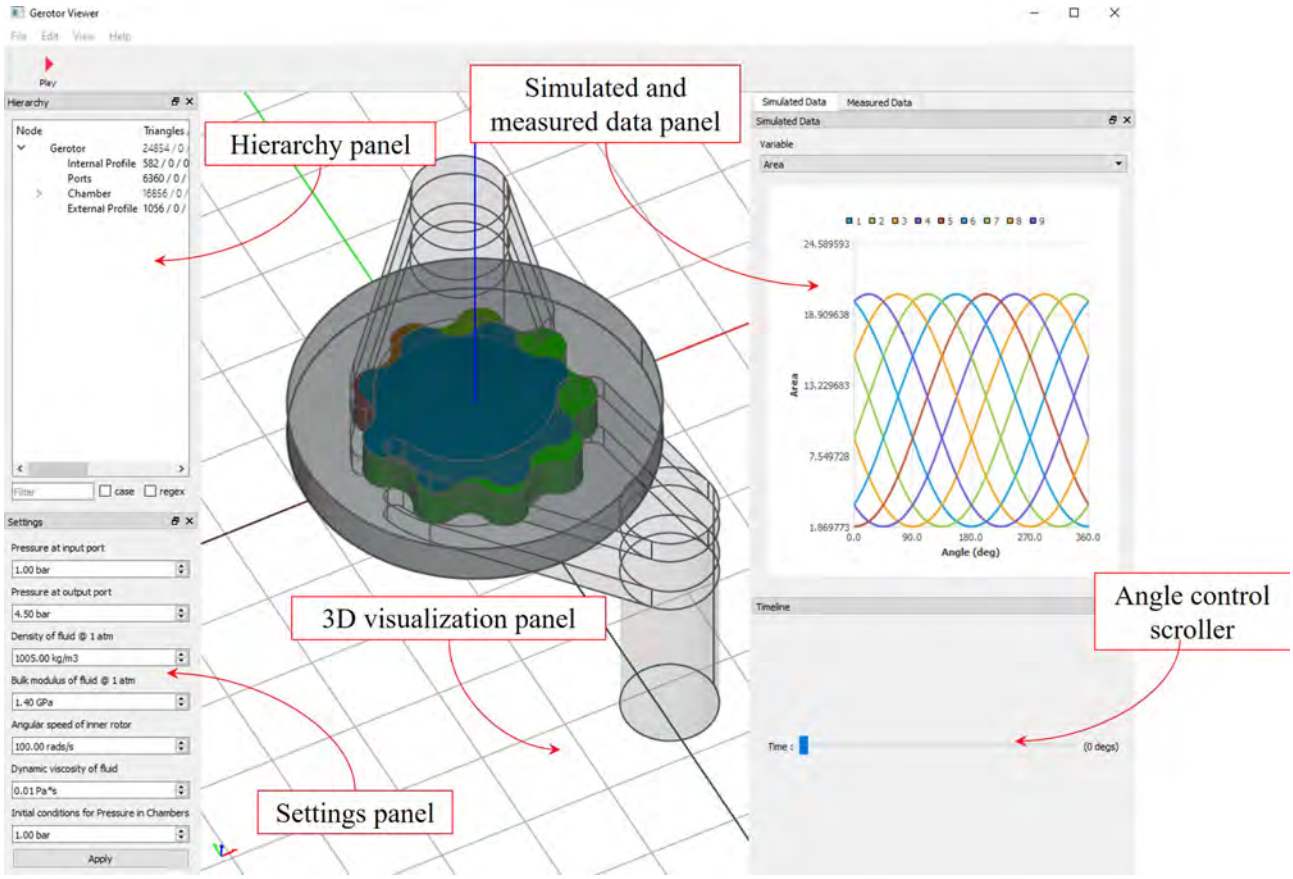

Figure 12. Three-dimensional (3D) data tool interface.

The 3D visualization panel enables design engineers to examine the three-dimensional behavior of the pumps for the parameters that are defined in the Geometry Configuration interface. Notice that the shape of the chambers must be recalculated each time the pump is set to a new angle position. Figure 13 shows the high degree of flexibility that can be achieved in the visualization of the different components of the pump geometry.

In Figure 13b, the color of each chamber is related to the pressure that is calculated by the simulation model. The tool also allows for the design engineer to import data from the CFD simulations and test bench tests with the objective of integrating and comparing performance data (both predicted and measured) in the same software environment. Figure 14 shows the data for a measured variable that was imported from an external CFD simulation, as visualized within the software tool. It is possible to import external data in the form of the widely used CSV format or while using a special text formatting that was specifically tuned for our application.

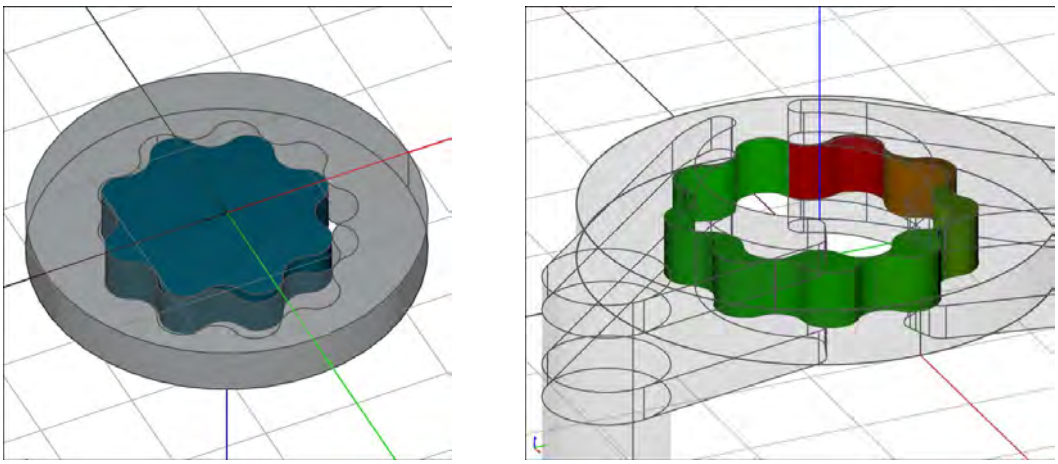

(**a**) (**b**)

Figure 13. Geometry visualization: (**a**) inner and outer gear of the pump, (**b**) fluid chambers with transparent ports.

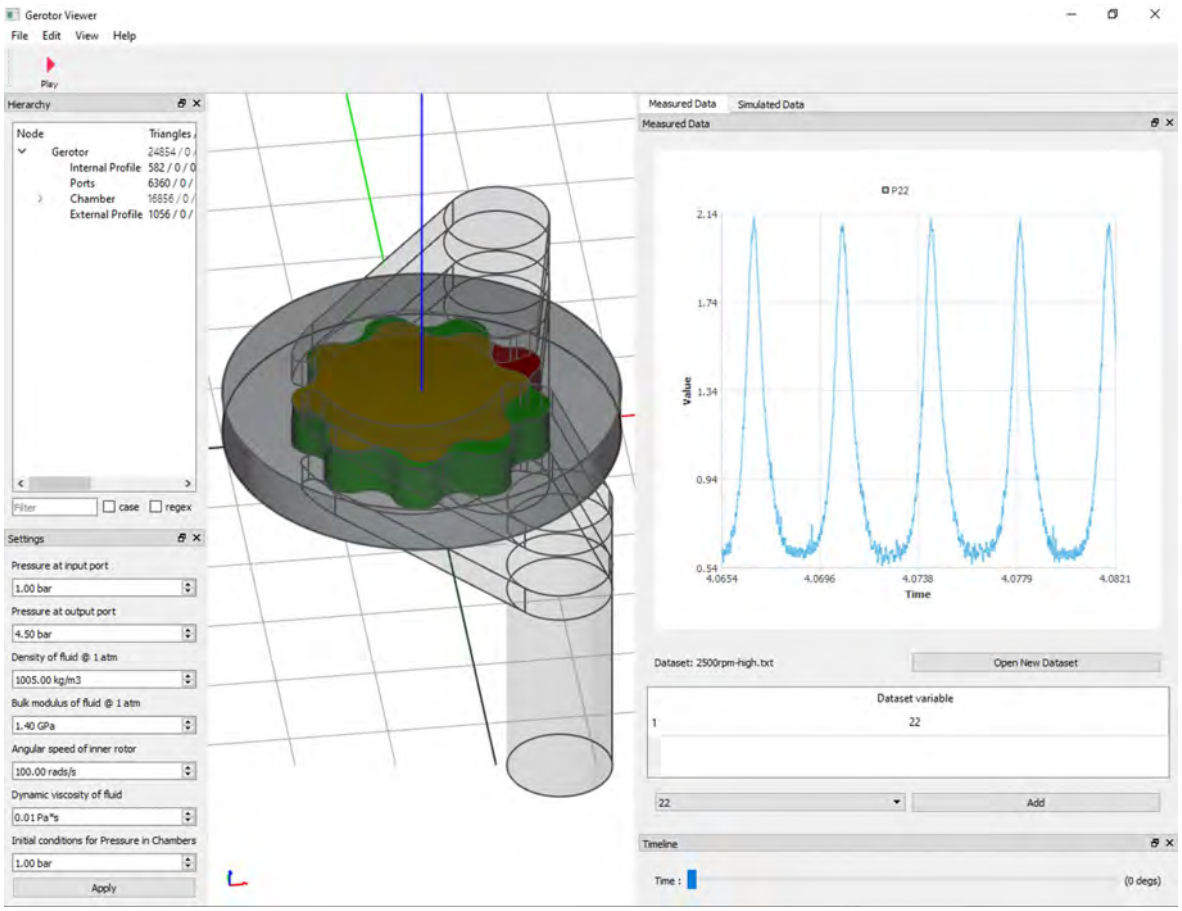

Figure 14. Example of the pressure data collected from the experimental setup sensors.

4. Results

We present the results of a design case while using the presented virtual prototype tool to design and simulate a gerotor pump. We also compare the obtained results with the data imported from an external CFD simulation for the same geometry, fluid properties, and operating conditions. Figures 15 and 16 present the volumetric data that were calculated by our tool for the pump design used in this test run.

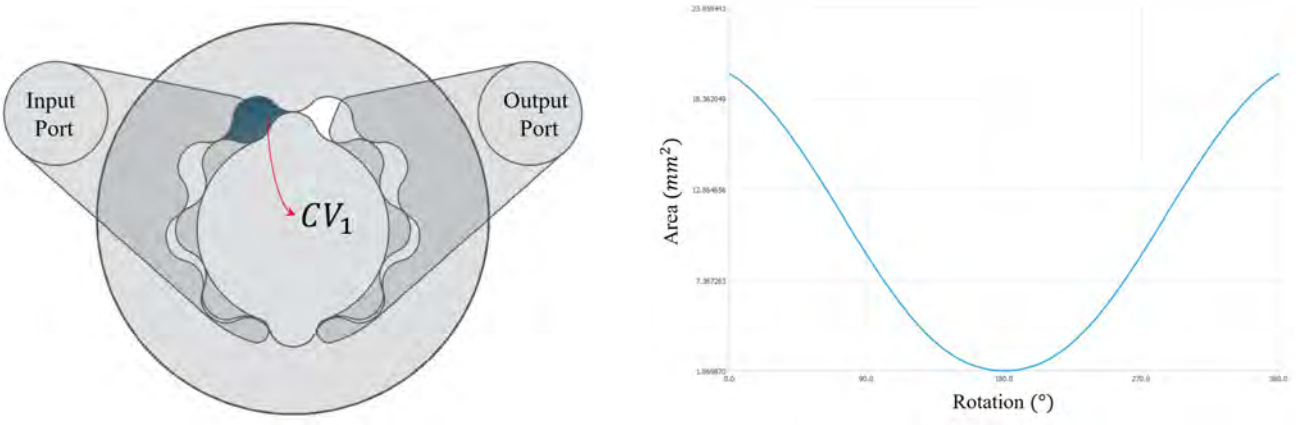

(**a**) (**b**)

Figure 15. Volumetric data results from the virtual prototype: (**a**) profile of geometry with highlighted chamber (CV_1) and (**b**) history of area in a z-cut for selected chamber.

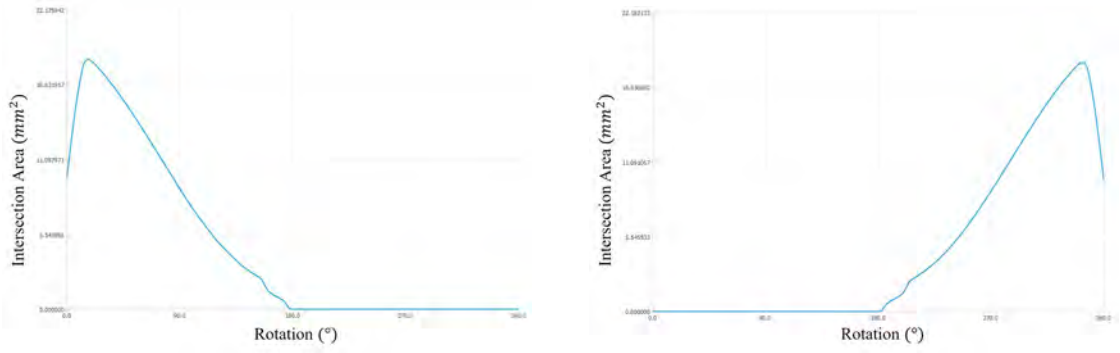

(**a**) (**b**)

Figure 16. Volumetric data results from the virtual prototype: (**a**) history of intersection area between chamber CV_1 and input port and (**b**) history of intersection area between chamber CV_1 and output port.

Figure 15a shows the selected analysis chamber. In this case, we have selected the maximum volume chamber when the pump is at initial position $t = 0$, even though our tool can perform the geometric analysis of all chambers simultaneously. Figure 15b shows the area evolution for the analysis chamber. Notice that it starts with the maximum value and diminishes until it reaches the minimum value for chamber area around halfway through a revolution. The minimum value for the area is not exactly zero because of the gaps in the meshing between the internal and external rotors described in the previous section. The area then rises until it reaches the maximum value once the revolution of the pump is completed. Figure 16a shows the intersection area between the analysis chamber and the input port (area through which the working fluid enters the pump). Notice that the intersection area increases at first, because, at initial position, the port and the chamber are only partially overlapped (as seen in Figure 15a). When the chamber is no longer overlapping with the input port and has started discharging fluid (overlapping with the output port), the intersection area with the input port becomes zero. The same analysis corresponds to the intersection area between the chamber and output port shown in Figure 16b. Figure 17 shows the history of areas for all chambers in the pump; the periodicity is explained by the cyclic design of the pump.

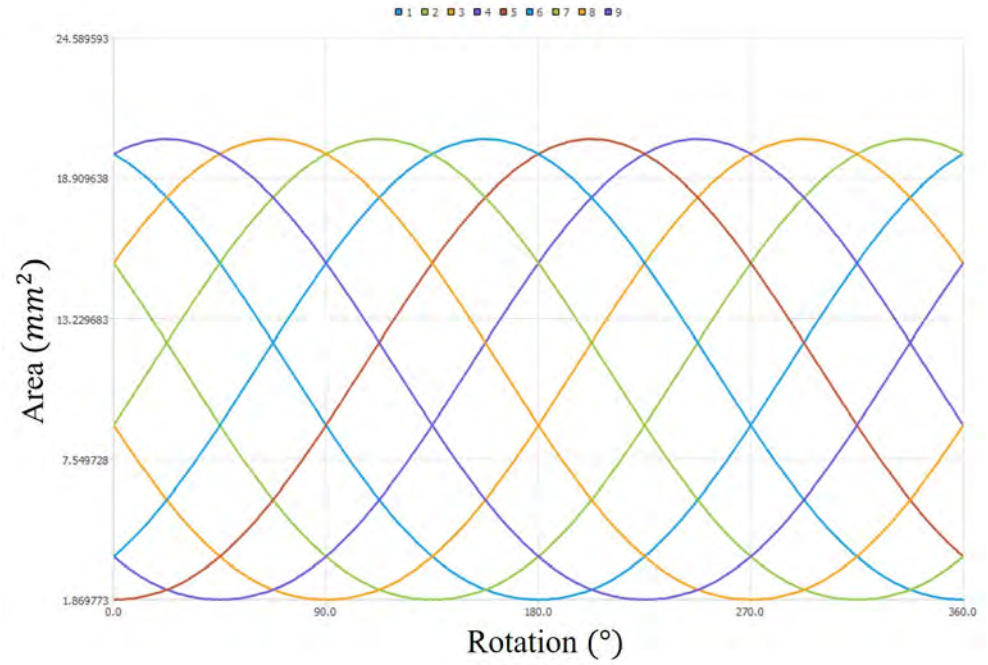

Figure 17. History of area for all 9 chambers in the pump.

We now discuss the results of a fluid dynamics simulation with our virtual prototype tool. The fluid properties, operating conditions and initial pressure conditions that are used for the simulation presented, are described in Table 1:

Table 1. Simulation conditions for test operating point.

Variable	Value	Units
Pressure at input port (p_{in})	1	bar
Pressure at output port (p_{out})	4.5	bar
Density of fluid at 1 atm (ρ_{oil})	1005	kg/m^3
Bulk modulus of fluid at 1 atm (β_{oil})	1.4	GPa
Angular speed of inner rotor (ω)	100	rad/s
Dynamic viscosity (μ)	0.01	Pa*s
Pressure in chambers at $t = 0$	1	bar

Figure 18 shows the history of calculated pressure inside an analysis chamber. Notice that the analysis chamber CV_1 (Figure 18a) is initially near the maximum volume position and, therefore, the initial pressure $P_{t=0}$ will be low (near input port pressure). As the pump rotates, the volume of the chamber reduces and increases the pressure inside the chamber. The maximum value of the pressure in chamber is reached in the minimum volume position and, once the analysis chamber enters the discharge cycle, the pressure starts to reduce as a result of the discharge of fluid and increase in volume of the chamber itself.

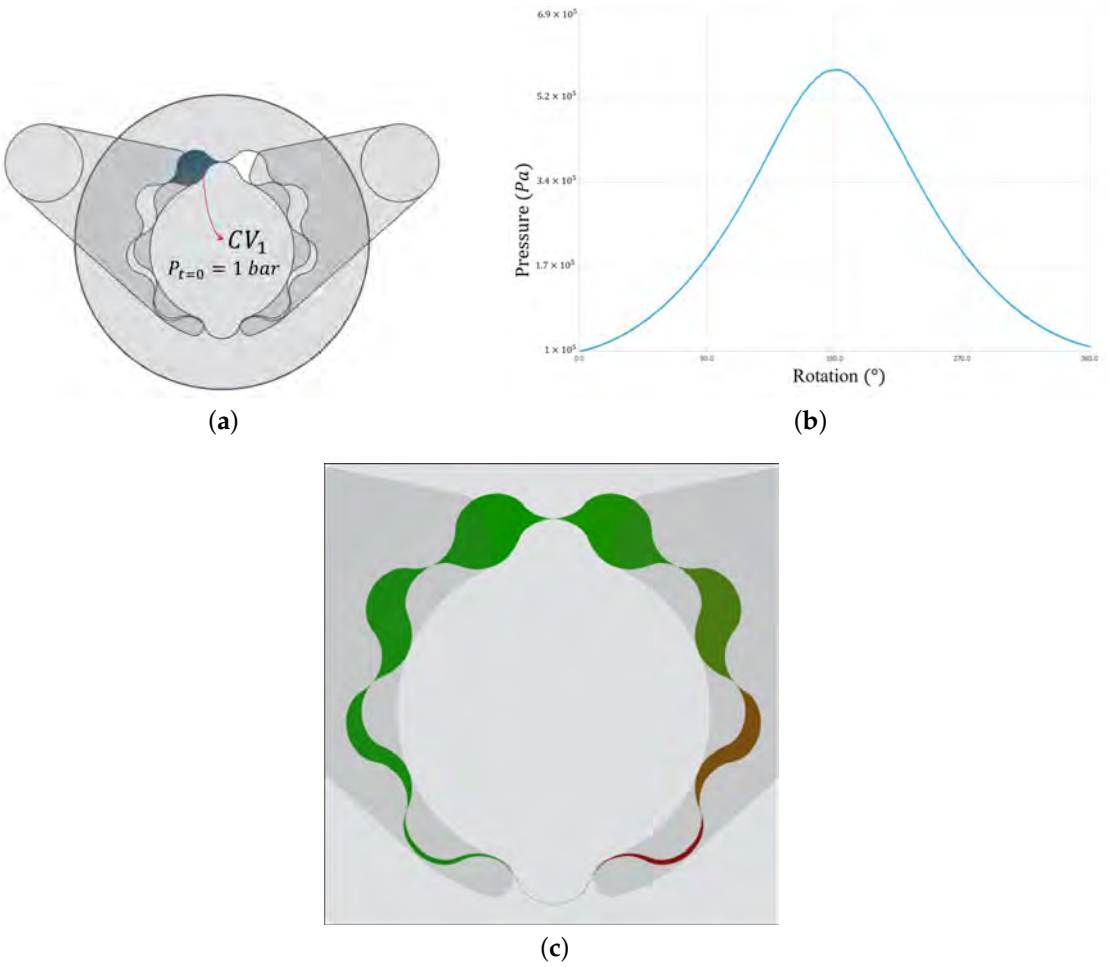

Figure 18. Pressure results from virtual prototype: (**a**) profile of geometry with highlighted chamber (CV_1), (**b**) history of pressure in chamber CV_1, and (**c**) pressure distribution in pump after a full revolution, as seen in Digital Twin (DT).

Figure 18c shows the pressure distribution in pump after a full revolution. Notice that there is a peak in pressure in the chambers near the minimum volume position and the pressure starts decreasing after the chamber intersects with the output port and goes through the discharge cycle. The discretization that was used in our virtual prototype allows for the tracking of the history of pressure for each individual chamber. However, the discretization used in the CFD methods make it impossible to track the history of pressure for an individual chamber. This is because, in CFD, the entire discretization (mesh) is updated in every time step (remeshing) to meet convergence requirements [21]. Therefore, for the purposes of comparison against a benchmark (i.e., CFD data), we use the maximal pressure across the entire fluid domain (all chambers). The CFD simulations are currently used in most of the design processes as an accurate prediction of the pump's performance. Therefore, they are a valid point of comparison for our implementation. Figure 19 shows the results of maximum pressure in pump, as predicted by both CFD simulation and by our implementation.

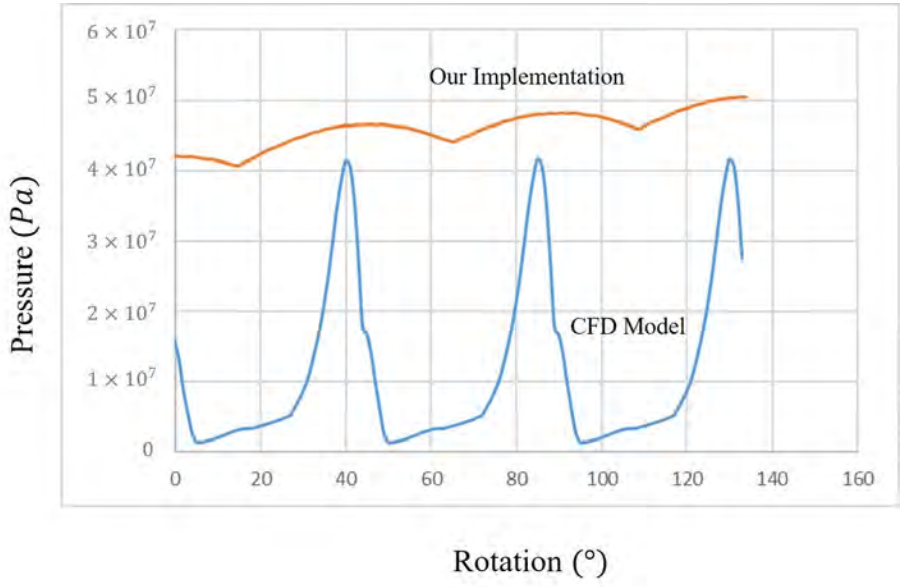

Figure 19. Virtual Prototype vs. computational fluid dynamics models (CFD) maximum predicted pressure in gerotor pump.

Our implemented virtual prototype is able to estimate the maximum pressure within the pump with a relative error of 21%. Our virtual prototype fails to reproduce the amplitude of the pressure oscillation in the pump. We believe that this shortcoming is due to the used assumption of homogeneous pressure in each one of the control volumes. The CFD model does not need such an assumption, and it is able to take into account variations of pressure within the chambers. Still, the maximum pressure in the pump as it rotates through an entire revolution is an important indication of the pump's performance, and it is reasonably estimated by our virtual prototype.

Table 2 shows a comparison of pre-processing and simulation times for both a CFD simulation and a simulation with our virtual prototype. The pre-processing time of the CFD simulation includes the generation of CAD models and mesh generation. The pre-processing time in our virtual prototype includes the parameter input for the geometry configuration tool and the automatic generation of B-Rep models. The main advantage of our virtual prototype is the much lower processing and simulation time, while still providing valuable performance information to the design engineer. The economic impact of our prototype upon the maker's functioning is not available at the present time, because of the fact that the design process, at the maker's facilities, is intertwined with other products and processes.

Table 2. Comparison of pre-processing and simulation times for the CFD simulation and our virtual prototype.

Task	CFD Time	Our Implementation Time
Pre-Processing of Geometry	1 h	<5 min
Simulation	9 h	<5 min

5. Conclusions and Future Work

In this manuscript, we have presented the implementation of a virtual prototype tool in the context of gerotor pump design, a component that has been widely used in different industries and that usually requires time-consuming tasks in the design workflow. Our implementation is a first step towards a fully functional Digital Twin of a gerotor pump. Our implemented tool allows for the integration of data that are collected from an experimental setup with a virtual prototype model. The collected data are fed to

the numerical model in order to improve the accuracy of the performance predictions. This allows the engineer to have a fast overview of the performance of the pump and allows him to discard unsuitable geometric configurations in an efficient manner. The presented implementation integrates a 2D design interface with an interactive parameterized model of the pump and a 3D interface. The 3D tool allows for the visualization of the 3D model that corresponds to the previously defined 2D geometry. Our initial tests show that the implemented model to perform fast pre-CFD simulations approaches the result of more detailed and time-consuming simulations within an acceptable margin of error. Our implemented tool also integrates, in a single application, the geometry data and simulation data, which are otherwise treated in different environments. Our virtual prototype is not suitable if a detailed prediction of the behavior inside each chamber of the pump is required.

Future work is needed in the improvement of both the software implemented and the fast simulation model in order to achieve a fully functional Digital Twin tool of the pump. Efforts regarding the 3D tool should be focused on data visualization and the creation of a data structure for simulation profiles of different geometric configurations. A needed improvement of the pre-CFD simulation may be achieved by modeling (a) cavitation and (b) micro-movements in the rotors, due to induced pressure at the chambers. A further integration of experimental data with the simulation model is needed to improve the accuracy of the predictions.

Author Contributions: J.P.-C., A.M., A.P.-B., E.S.-J. and O.R.-S. conceptualized the tool; J.P.-C., A.M. and B.S. implemented the tool; J.P., O.R.-S., E.S.-J. and A.P.-B. supervised the industrial application of the tool; A.M., B.S. and J.P.-C. implemented the geometrical aspects of this research; J.P.-C., E.S.-J. and A.P.-B. supervised the simulation model results. All the authors contributed to the writing of the article. All authors have read and agreed to the published version of the manuscript.

Funding: This work has received funding from the Eusko Jaurlaritza/Basque Government under the grants KK-2018/00071 (LANGILEOK) and ZL-2020/00190 (LATIDO).

Acknowledgments: The authors thank Tecnun-Universidad de Navarra for the support in the CFD-generated operational data.

Conflicts of Interest: The authors declare no conflict of interest.

Abbreviations

LP	Lumped Parameter.
CFD	Computational Fluid Dynamics.
P_i	Pressure at chamber i.
A_i	Area at chamber i.
V_i	Volume at chamber i.
Q_i	Net flowrate at chamber i.
$A_{i,out}$	Shared area between chamber i and output port.
$A_{i,in}$	Shared area between chamber i and input port.
C_d	Discharge coefficient.
$C_{d,max}$	Maximum discharge coefficient.
β_{eff}	Effective bulk's modulus of working fluid.
ρ_{eff}	Effective density of working fluid.
ν	Kinematic viscosity of working fluid.
μ	Dynamic viscosity of working fluid.
Re	Reynold's number.
Re_{crit}	Critical Reynold's number.
Dh	Hydraulic diameter.
p_{in}	Pressure at input port.
p_{out}	Pressure at output port.
ω	Angular speed of inner gear.

References

1. Gamez-Montero, P.J.; Codina, E.; Castilla, R. A review of gerotor technology in hydraulic machines. *Energies* **2019**, *12*, 2423. [CrossRef]
2. Castilla, R.; Gamez-Montero, P.; Ertürk, N.; Vernet, A.; Coussirat, M.; Codina, E. Numerical simulation of turbulent flow in the suction chamber of a gearpump using deforming mesh and mesh replacement. *Int. J. Mech. Sci.* **2010**, *52*, 1334–1342. [CrossRef]
3. Houzeaux, G.; Codina, R. A finite element method for the solution of rotary pumps. *Comput. Fluids* **2007**, *36*, 667–679. [CrossRef]
4. Hsieh, C.F. Fluid and dynamics analyses of a gerotor pump using various span angle designs. *J. Mech. Des.* **2012**, *134*. [CrossRef]
5. Bae, J.H.; Kwak, H.S.; San, S.; Kim, C. Design and CFD analysis of gerotor with multiple profiles (ellipse–involute–ellipse type and 3-ellipses type) using rotation and translation algorithm. *Proc. Inst. Mech. Eng. Part C J. Mech. Eng. Sci.* **2016**, *230*, 804–823. [CrossRef]
6. Rundo, M.; Altare, G. Lumped Parameter and Three-Dimensional CFD Simulation of a Variable Displacement Vane Pump for Engine Lubrication. *J. Fluids Eng.* **2018**, *140*, 61–101. [CrossRef]
7. Gamez-Montero, P.J.; Castilla, R.; del Campo, D.; Ertürk, N.; Raush, G.; Codina, E. Influence of the interteeth clearances on the flow ripple in a gerotor pump for engine lubrication. *Proc. Inst. Mech. Eng. Part D J. Automob. Eng.* **2012**, *226*, 930–942. [CrossRef]
8. Pellegri, M.; Vacca, A.; Frosina, E.; Buono, D.; Senatore, A. Numerical analysis and experimental validation of Gerotor pumps: A comparison between a lumped parameter and a computational fluid dynamics-based approach. *Proc. Inst. Mech. Eng. Part C J. Mech. Eng. Sci.* **2017**, *231*, 4413–4430. [CrossRef]
9. Pellegri, M.; Vacca, A.; Devendran, R.S.; Dautry, E.; Ginsberg, B. A Lumped parameter approach for gerotor pumps: Model Formulation and experimental validation. In Proceedings of the 2016 10th International Fluid Power Conference, Dresden, Germany, 8–10 March 2016; Technische Universitat Dresden: Dresden, Germany, 2016; Volume 1, pp. 465–476.
10. Shah, Y.; Vacca, A.; Dabiri, S.; Frosina, E. A fast lumped parameter approach for the prediction of both aeration and cavitation in Gerotor pumps. *Meccanica* **2018**, *53*, 175–191. [CrossRef]
11. Rundo, M. Models for flow rate simulation in gear pumps: A review. *Energies* **2017**, *10*, 1261. [CrossRef]
12. Tao, F.; Zhang, H.; Liu, A.; Nee, A.Y. Digital twin in industry: State-of-the-art. *IEEE Trans. Ind. Inform.* **2018**, *15*, 2405–2415. [CrossRef]
13. Pires, F.; Cachada, A.; Barbosa, J.; Moreira, A.P.; Leitão, P. Digital Twin in Industry 4.0: Technologies, Applications and Challenges. In Proceedings of the 2019 IEEE 17th International Conference on Industrial Informatics (INDIN), Espoo, Finland, 22–25 July 2019; IEEE: Piscataway, NJ, USA, 2019; Volume 1, pp. 721–726.
14. Mejia, D.; Moreno, A.; Arbelaiz, A.; Posada, J.; Ruiz-Salguero, O.; Chopitea, R. Accelerated thermal simulation for three-dimensional interactive optimization of computer numeric control sheet metal laser cutting. *J. Manuf. Sci. Eng.* **2018**, *140*. [CrossRef]
15. Mejia-Parra, D.; Arbelaiz, A.; Ruiz-Salguero, O.; Lalinde-Pulido, J.; Moreno, A.; Posada, J. Fast Simulation of Laser Heating Processes on Thin Metal Plates with FFT Using CPU/GPU Hardware. *Appl. Sci.* **2020**, *10*, 3281. [CrossRef]
16. Gámez Montero, P.J. *Caracterizacion Fluidodinamica de una Bomba Oleohidráulica de Engranajes Internos Generados por Perfiles Trocoidales*; Universitat Politècnica de Catalunya: Barcelona, Spain, 2004.
17. Kwon, S.M.; Kang, H.S.; Shin, J.H. Rotor profile design in a hypogerotor pump. *J. Mech. Sci. Technol.* **2009**, *23*, 3459–3470. [CrossRef]
18. Kim, S.; Murrenhoff, H. Measurement of effective bulk modulus for hydraulic oil at low pressure. *J. Fluids Eng.* **2012**, *134*. [CrossRef]
19. Simões, B.; Creus, C.; Carretero, M.d.P.; Guinea Ochaíta, A. Streamlining XR Technology Into Industrial Training and Maintenance Processes. In *The 25th International Conference on 3D Web Technology*; Association for Computing Machinery: New York, NY, USA, 2020. [CrossRef]
20. Simões, B.; del Puy Carretero, M.; Santiago, J.M. Photorealism and Kinematics for Web-Based CAD Data. In *The 25th International Conference on 3D Web Technology*; Association for Computing Machinery: New York, NY, USA, 2020. [CrossRef]
21. Castilla López, R.; Gámez Montero, P.J.; Raush Alviach, G.A.; Codina Macià, E. Three dimensional simulation of gerotor with deforming mesh by using OpenFOAM. In Proceedings of the Fluid Power Networks: Proceedings: 19th-21th March 2018: 11th International Fluid Power Conference, Aachen, Germany, 19–21 March 2018; pp. 260–271.